


Controlling the polarization and phase of high-order harmonics with a plasmonic metasurface: supplement

SOHAIL A. JALIL,¹ KASHIF M. AWAN,² IDRIS A. ALI,¹ SABAA RASHID,³ JOSHUA BAXTER,^{3,4} ALEKSEY KOROBENKO,¹  GUILMOT ERNOTTE,¹ ANDREI NAUMOV,¹ DAVID M. VILLENEUVE,¹ ANDRÉ STAUDTE,¹ PIERRE BERINI,^{3,4,5}  LORA RAMUNNO,^{3,4} AND GIULIO VAMPA^{1,*}

¹Joint Attosecond Science Laboratory, National Research Council of Canada and University of Ottawa, Ottawa, Ontario K1N 0R6, Canada

²Stewart Blusson Quantum Matter Institute, University of British Columbia, Vancouver, British Columbia V6T 1Z4, Canada

³Centre for Research in Photonics, University of Ottawa, 25 Templeton Street, Ottawa, Ontario K1N 6N5, Canada

⁴Department of Physics, University of Ottawa, 150 Louis Pasteur, Ottawa, Ontario K1N 6N5, Canada

⁵School of Electrical Engineering and Computer Science, University of Ottawa, 800 King Edward Avenue, Ottawa, Ontario K1N 6N5, Canada

*Corresponding author: gvampa@uottawa.ca

This supplement published with Optica Publishing Group on 24 August 2022 by The Authors under the terms of the [Creative Commons Attribution 4.0 License](https://creativecommons.org/licenses/by/4.0/) in the format provided by the authors and unedited. Further distribution of this work must maintain attribution to the author(s) and the published article's title, journal citation, and DOI.

Supplement DOI: <https://doi.org/10.6084/m9.figshare.20449191>

Parent Article DOI: <https://doi.org/10.1364/OPTICA.464445>

Controlling polarization and phase of high-order harmonics with a plasmonic metasurface

Sohail A. Jalil¹, Kashif M. Awan², Idriss A. Ali¹, Sabaa Rashid³, Joshua Baxter^{3,4}, Aleksey Korobenko¹, Guilmot Ernotte¹, Andrei Naumov¹, David M. Villeneuve¹, André Staudte¹, Pierre Berini^{3,4,5}, Lora Ramunno^{3,4}, Giulio Vampa^{1*}

¹ Joint Attosecond Science Laboratory, National Research Council of Canada and University of Ottawa, Ottawa, Ontario, K1N 0R6, Canada

² Stewart Blusson Quantum Matter Institute, University of British Columbia, Vancouver, British Columbia V6T 1Z4, Canada

³ Centre for Research in Photonics, University of Ottawa, 25 Templeton Street, Ottawa, Ontario K1N 6N5, Canada

⁴ Department of Physics, University of Ottawa, 150 Louis Pasteur, Ottawa, Ontario K1N 6N5, Canada

⁵ School of Electrical Engineering and Computer Science, University of Ottawa, 800 King Edward Avenue, Ottawa, Ontario K1N 6N5, Canada

*gvampa@uottawa.ca

1. Design of rectangular nano-antenna arrays.

Figure S1, shows the sketch of rectangular antennas, placed on 500 nm thick silicon film on sapphire substrate. The arrays of these antennas are symmetric in x and y axes. A unit cell of $450 \times 450 \text{ nm}^2$ with periodic boundary conditions in x and y planes, and perfectly matched layer in z-plane are simulated by solving Maxwell's equations numerically, using the finite difference time domain method from Lumerical® with a mesh of $1 \times 1 \times 1 \text{ nm}^3$. Two plane-waves with orthogonal polarization with a relative phase-delay of 90° having an electric field magnitude of 1 V/m, located inside sapphire substrate, illuminates the arrays from below at normal incidence. The refractive indices of sapphire, silicon and gold were obtained from Palik's material data [1]. The individual rectangular antenna was 195 nm long, 80 nm wide and 20 nm thick with a gap of 30 nm. The transmittance (T) ($4 \mu\text{m}$ above the antennas) and reflectance ($4 \mu\text{m}$ below the antennas) were computed as a function of wavelength at reference planes. The total absorptance (A) was calculated according to this relation: $A = 1 - T - R$.

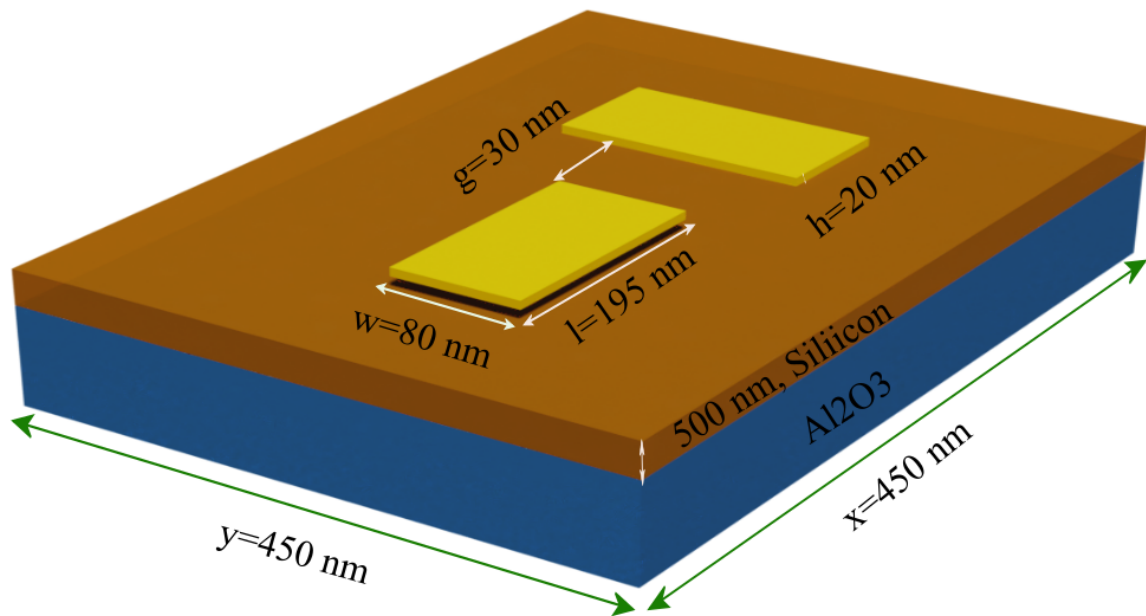


Fig. S1. The geometry of the unit cell of the simulated structure. The perpendicular rectangular antennas are placed on 500 nm thick silicon film, on sapphire substrate. A circularly-polarized light is shined from below through sapphire substrate.

Figure S2 (**panel a**) shows the absorptance as a function of the wavelength calculated using the above equation from the unit cell with geometrical parameters shown above. The spatial magnitude of electric field distribution of the enhancement along a cut 5 nm below the Si surface is plotted in Figure S2 (**panel b**), for circular polarization. Enhancement is achieved when circular polarization is parallel to the major axis of the antennas. The excitation of a surface plasmon polariton mode of the nano-antennas converts far-field radiation into intense localized near-fields which enhance high harmonic generation.

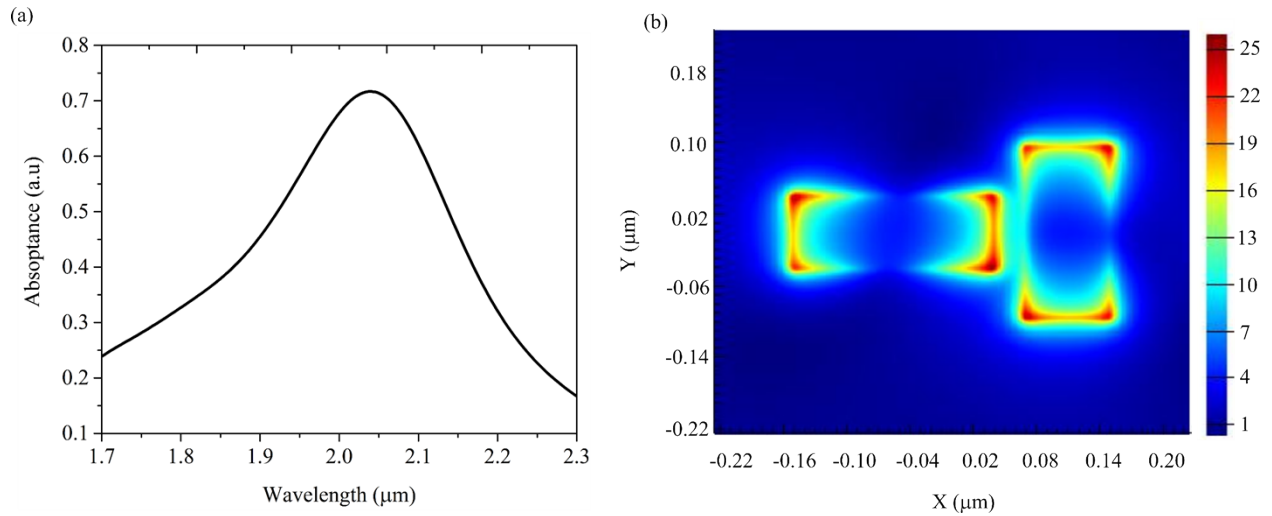


Fig. S2. (a) The absorptance as a function of wavelength is obtained from the reflectance and transmittance monitors. (b) The magnitude of electric field in the x-y plane 5 nm inside Silicon, for perpendicular antennas of dimensions $L=195$ nm, $W=80$ nm, $\text{gap}=30$ nm, $\text{pitch}=450 \times 450$ nm², at $\lambda = 2050$ nm, which is the resonance wavelength (a).

2. Fabrication of the nanoantenna arrays.

Figure 2 (inset) shows a scanning electron image of a nano-antenna array, wherein orthogonal rectangular antennas are fabricated by electron-beam lithography followed by metal evaporation and lift-off on the surface of a 500-nm-thick single-crystal silicon film. Several arrays (70×70 μm^2 area) of perpendicular nano-antennas are fabricated to ensure that the optimal dimensions required at the resonant wavelength are met for a subset of these arrays. The silicon film is grown on an R-plane 500-nm-thick sapphire substrate (MTI Corp.). Diced chips are cleaned using acetone and IPA, and then blow-dried using nitrogen. A 2% weight PMMA in anisole solution, with a molecular weight of 450k, is used for the bottom resist layer. The diced samples are spin-coated at 5000 rpm for 60 seconds with an acceleration of 1000 rps, and then baked at 180 $^{\circ}\text{C}$ for 30 minutes, which resulted in a 50-nm-thick bottom resist layer. Similarly, a 2% wt PMMA in anisole solution, with a molecular weight of 950k, is used for the top resist layer. The top layer is spin-coated at 7000 rpm for 60 seconds, with an acceleration of 300 rps, which resulted in a 25-nm-thick top resist layer. A bilayer resist stack is used to create a re-entrant profile ensuring clean lift-off of the metal features. The nano-antennas are patterned by electron-beam lithography with a dose of $360 \mu\text{Ccm}^{-2}$. The samples are developed in MIBK/IPA 1:3 at 20 $^{\circ}\text{C}$ for 60 seconds. A 0.5 nm-thick titanium adhesion layer is deposited directly on the substrate followed by the evaporation of 20 nm of gold, both using electron-beam evaporation. As a final fabrication step, the metal lift-off takes place in an acetone bath at room temperature, which is sonicated at 30 kHz for 30 seconds and followed by blow-dried using nitrogen.

3. Measuring the Stokes parameters by rotating quarter-waveplate ($\lambda/4$) method.

In order to confirm that the generated harmonics are circularly-polarized rather than unpolarized, we adopted the rotating quarter wave plate method [2] to retrieve the Stokes parameters for the 5th harmonic. For this purpose, we used a $\lambda/4$ waveplate and a polarizer after the sample and measured the harmonic intensity of HH5 as a function of

the waveplate angle. A plot of the measured HH5 intensity as a function of the waveplate angle, θ , is shown in **Figure S3**.

The intensity of the harmonic beam I_n that is transmitted through the waveplate-polarizer combination for each waveplate angle θ_n , can be written as [2]:

$$I_n = \frac{1}{2}(A + B \sin 2\theta_n + C \cos 4\theta_n + D \sin 4\theta_n) \quad (n = 1, 2, 3 \dots N) \quad (1)$$

The coefficients A, B, C and D are determined using:

$$A = \frac{2}{N} \sum_{n=1}^N I_n, \quad B = \frac{4}{N} \sum_{n=1}^N I_n \sin 2\theta_n, \quad C = \frac{4}{N} \sum_{n=1}^N I_n \cos 4\theta_n, \quad D = \frac{4}{N} \sum_{n=1}^N I_n \sin 4\theta_n \quad (2)$$

By substituting the experimental harmonic intensities I_n into (2), we obtain the values of the coefficients $A = 3689.067$, $B = -3551.469$, $C = -442.142$, and $D = 297.220$.

The Stokes parameters are found to be:

$$S_0 = A - C, \quad S_1 = 2C, \quad S_2 = 2D, \quad S_3 = B.$$

This procedure yields the normalized Stokes vector as:

$$S = \begin{pmatrix} 1 \\ -0.214 \\ 0.144 \\ -0.860 \end{pmatrix}$$

This confirms that HH5 is 90% polarized, and is primarily left circularly polarized.

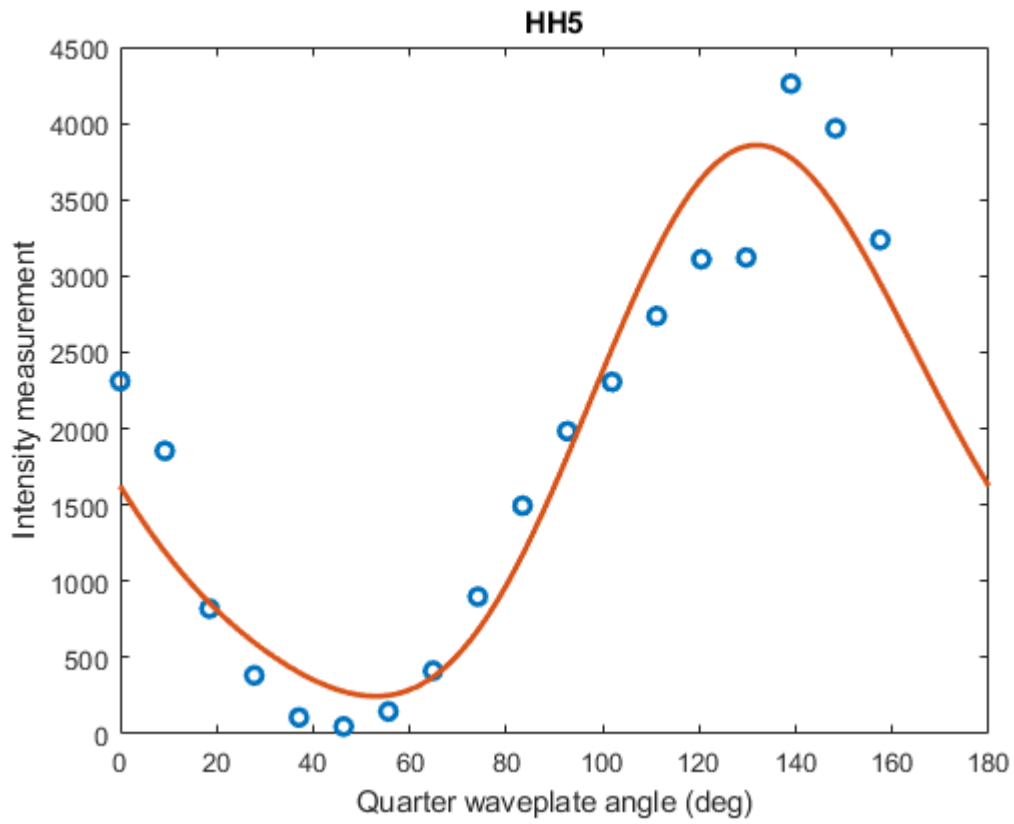


Fig. S3. Measured intensity of HH5 after passing through a polarization analyzer composed of a quarter waveplate and a linear polarizer, as a function of the angle of the quarter waveplate (circles). The line is a fit to the data using eqs. 1 and 2.

References

1. Palik, E. D. *Handbook of optical constants of solids*. Vol. 3 (Academic press, 1998).
2. Schaefer, B., Collett, E., Smyth, R., Barrett, D. & Fraher, B. Measuring the Stokes polarization parameters. *American Journal of Physics* **75**, 163-168 (2007).